JOURNAL OF THEORETICAL
AND APPLIED MECHANICS
1, 36, 1998

PARAMETRIC STUDY OF A PNEUMATIC TIRE UNDER INFLATION USING THE FEM APPROACH

JÓZEF PELC

Department of Mechanical Engineering, Olsztyn University of Agriculture and Technology
e-mail: joseph@moskit.art.olsztyn.pl

The influence of some structural parameters of a pneumatic tire on its deformation and stresses under inflation pressure has been analyzed. The 2D axisymmetrical finite element model was applied. Large displacements have been taken into account in the strain-displacement relations. Orthotropy ratio variations appearing in a specific tire cord-rubber composite have been also considered. The following input data have been taken: belt ply width, belt cord angle and longitudinal stiffness of carcass fiber. The tire model was verified using the experimental results. Good correlation was observed between the corresponding displacements.

Key words: tire, composite materials, finite element modelling

1. Introduction

A lot of attempts have been made to utilize computational models of a tire in the improvement of its design process. A survey of various tire models and a long reference list may be found in Ridha (1980) and Pelc (1991). Today, the finite element method (FEM) is considered as a unique and powerful tool for the structural analysis of pneumatic tires (Noor and Tanner, 1985). The reliable results obtained using this method have been successfully applied to the tire design process.

Drawbacks of other methods, when compared to the FEM, in solving the tire analysis problems appear due to heterogeneity, layered structure, limpness in initial configuration, cord anisotropy, large strains, material non-linearity and rubber incompressibility. In addition, the analysis of a tire subjected to a service loading requires the contact phenomenon to be considered. In mechanics of deformable solids such an object is classified as a highly non-linear composite structure.

In this paper the considerations are confined to an axisymmetric structure subjected to the inflation pressure only. Large displacements are taken into account in the strain-displacement relations. Plies are assumed to be made of orthotropic and linear elastic material (Pelc, 1992, 1994). Variations of the orthotropy ratio, due to the forming process which runs from building drums to the final configuration of a tire, are also considered.

Our finite element program, adapted for a 2D axisymmetric tire model, was used in the analysis of a passenger car radial tire. The effects of belt width, carcass fiber stiffness and belt cord angle variations on the inflated tire profile, displacements of two control points of the profile and the distribution of cord forces were examined.

The results of computations have been used in attempts at the improvement of performance parameters of a tire.

2. Radial tire construction

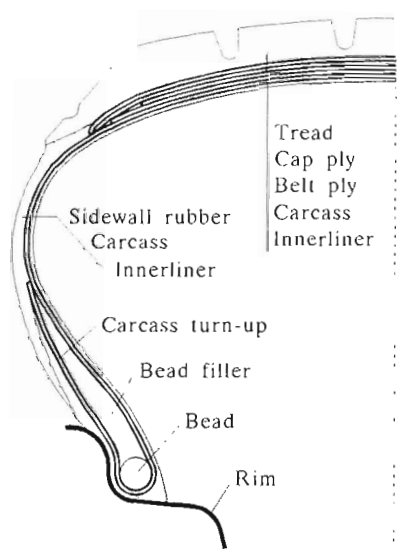

Fig. 1. Structural components of a passenger car pneumatic tire

The structural components of a passenger car pneumatic radial tire are shown in Fig.1. Tire is a specific composite structure. There are different mechanical properties of layered material at any location in the tire. This

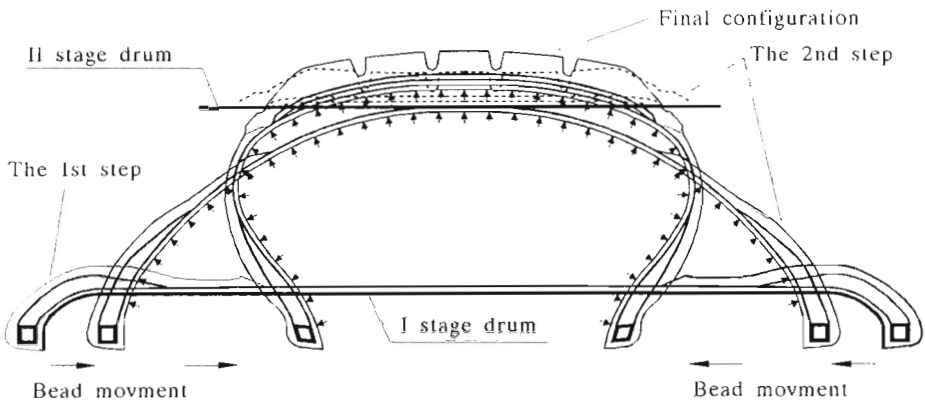

Fig. 2. Stages of the manufacturing process of a radial tire

is the effect of tire manufacturing process (Fig.2). In the process green tire constituent parts are set up on tire building drums. At subsequent stages the cord end count (ends per decimeter) and its angle to the drum parallel lines are constant in the cord-rubber layers. When the tire is being formed its beads are being moved axially towards the drum symmetry plane while the drum points are being shifted in radial direction. This causes the variations in the cord end count and its angles to parallels of a created toroidal shell. Hence, variations of the orthotropy ratio appear to be characteristic for the tire cord-rubber composite and making, therefore, the tire structural analysis extremely complicated. Fortunately, the cord angle θ measured from parallel lines at a distance r from the tire axis in its finite configuration can be expressed by the so-called pantographing role (DeEskinazi and Ridha, 1982)

$$\cos\theta = \frac{r}{r_C}\cos\theta_C \tag{2.1}$$

where the index C denotes the values measured at the maximum distance from the tire axis (at crown). In view of Eq (2.1) the cord end count i at any location r of a point within an expanded cord-rubber layer can be written as

$$i = i_C \frac{r_C \sin\theta_C}{r\sin\theta} \tag{2.2}$$

The cord-rubber layers layout in the tire to be analyzed is shown in Fig.3.

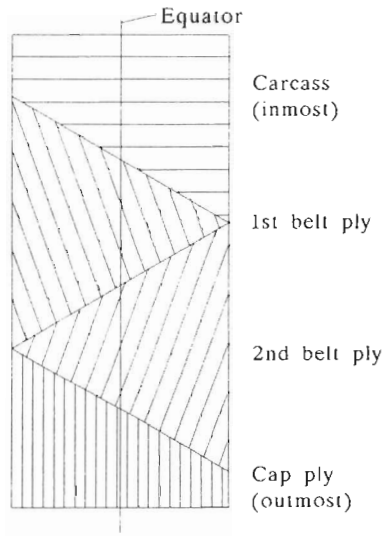

Fig. 3. Cord-rubber plies layout on the tire building drums

3. Computational model characteristic

A tire subjected to the inflation pressure usually undergoes the deformation characterized by the moderate strains in its components. Hence a linear relation between stresses and strains may be assumed. The material of rubber elements is assumed to be isotropic and almost incompressible (the Poisson ratio $\nu = 0.48$). The material of cord-rubber plies is considered as orthotropic and linear elastic. The stress-strain relations for the material are given below

$$\boldsymbol{S} = \frac{1}{V}\begin{bmatrix} E_1(1-\nu_{23}\nu_{32}) & E_2(\nu_{12}+\nu_{13}\nu_{32}) & 0 & E_3(\nu_{13}+\nu_{12}\nu_{23}) & 0 & 0 \\ & E_2(1-\nu_{13}\nu_{31}) & 0 & E_2(\nu_{23}+\nu_{21}\nu_{13}) & 0 & 0 \\ & & VG_{12} & 0 & 0 & 0 \\ & & & E_3(1-\nu_{12}\nu_{21}) & 0 & 0 \\ & \text{sym} & & & VG_{13} & 0 \\ & & & & & VG_{23} \end{bmatrix} \boldsymbol{E} \tag{3.1}$$

where

$$V = 1 - \nu_{12}\nu_{21} - \nu_{13}\nu_{31} - \nu_{23}\nu_{32} - \nu_{12}\nu_{23}\nu_{31} - \nu_{21}\nu_{13}\nu_{32}$$

and

$\boldsymbol{S}$ – 2nd Piola-Kirchhoff stress vector

$\boldsymbol{E}$ – Green-Lagrange strain vector.

The indices 1, 2 and 3 denote the fiber direction, axis perpendicular to the fiber coplanar to the ply and axis perpendicular to the latter two axes, respectively. Because the analysis is carried out in the (x, y, φ) coordinate system the constitutive matrix undergoes the transformation twice (cf Pelc, 1992). The effective material constants for a single ply E_1, E_2, G_{12} and ν_{12} may be predicted from the Halpin-Tsai equations (Walter and Patel, 1979)

$$E_1 = E_c v_c + E_r(1 - v_c) \qquad E_2 = \frac{E_r(1 + 2v_c)}{1 - v_c}$$

$$G_{12} = \frac{G_r[G_c + G_r + (G_c - G_r)v_c]}{G_c + G_r - (G_c - G_r)v_c} \tag{3.2}$$

$$\nu_{12} = \nu_c v_c + \nu_r(1 - v_c) \qquad \nu_{21} = \frac{\nu_{12} E_2}{E_1}$$

where

E_c, E_r – Young moduli of cord and rubber, respectively
G_c, G_r – shear moduli of cord and rubber, respectively
ν_c, ν_r – Poisson ratios of cord and rubber, respectively
v_c – volume fraction of cord in the ply.

Also it occurs: $\nu_{ij} E_j = \nu_{ji} E_i$, $i, j = 1, 2, 3$ and $i \neq j$. Additional equalities were assumed $E_3 = E_2$, $\nu_{13} = \nu_{12}$, $G_{13} = G_{12}$ and $G_{23} = 2G_{12}$.

The passenger car tire under consideration consists of steel cord belt plies, nylon cord cap plies and rayon cord carcass. To determine mechanical properties of cord-rubber plies, which vary from point to point in a cured tire, the input data for each ply were taken: ply thickness, cord fiber cross-sectional area, cord end counts per decimeter in the ply on the building drum, ply radius on the drum, Young moduli and Poisson ratios for rubber and cord. Using of Eqs (2.1) and (2.2) allows for taking into account variations of the cord angle and the cord end count, respectively, along the profile of a cured tire.

A finite element mesh and boundary conditions for the model are shown in Fig.4. The FEM tire model construction was supported by some special purpose pre-processing tools (Pelc, 1995). Innerliner (pure rubber) and carcass plies (cord-rubber) were stacked and modeled by one element only. For each element, mechanical properties of the material were calculated as weighted mean values with respect to the thicknesses of the components. In order to reduce a total number of elements the belt and cap plies were treated in the same way. The total number of 192 elements (33 six-node-ones and 159 eight-node-ones), 649 nodes, four types of layered and six kinds of isotropic materials, respectively, were used.

An incremental technique is most frequently used for solving non-linear equations governing the problem, in which large displacements, large strains

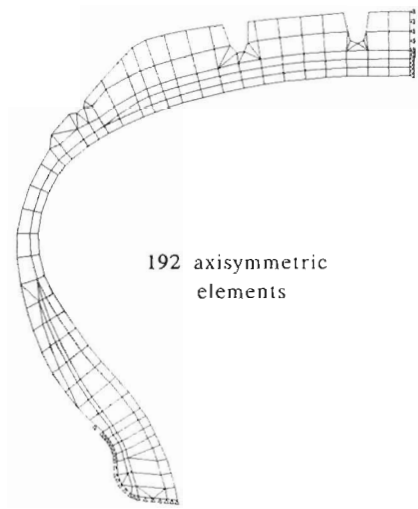

Fig. 4 Finite element mesh

and non-linear constitutive relations appear (Bathe, 1982). After the equations have been linearised the displacement increments caused by consecutive load increments may be calculated. If the initial configuration of the structure under consideration is known an approximate equilibrium path may be constructed. To avoid divergence from the exact solution the vectors of corrections are calculated in an iterative process for each load increment. The iteration is continued until the corrections are sufficiently small. The stiffness matrix of the structure is updated only once per load increment (modified Newton-Raphson procedure).

The modified constant arc length procedure proposed by Crisfield (1981) has appeared to be very useful in the solving process control. The procedure automatically increases load steps depending on the rate of convergence.

4. Verification of the model reliability

Whenever a true object is to be represented by a computational model, verification of the model reliability is required. In the case under consideration the displacements were measured at several points of the tire inflated up to 250 kPa. The results of measurement and computations are shown in Fig.5.

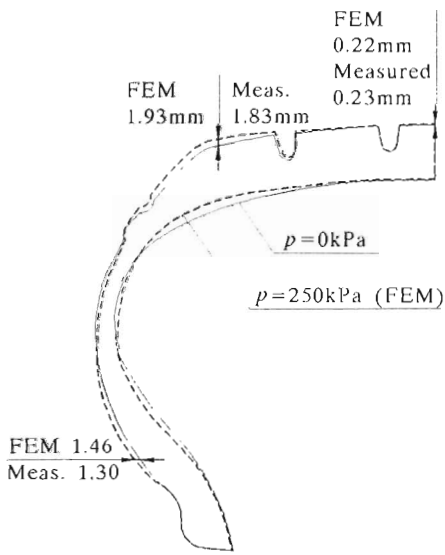

Fig. 5. Computed and measured displacements of the tire points

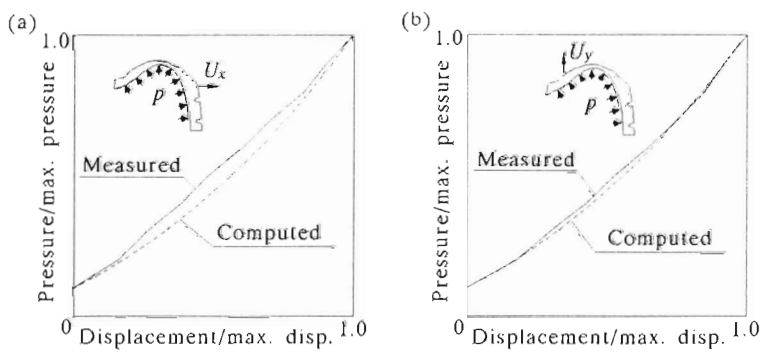

Fig. 6. Radial (a) and axial (b) displacements versus history plot of pressure

The equilibrium paths (pressure versus displacement) for two outer profile points of the tire have been traced too (cf Fig.6).

Comparing the experimental results with those obtained using the tire model a good correlation between the results of displacements is observed.

5. Numerical results for the passenger car tire

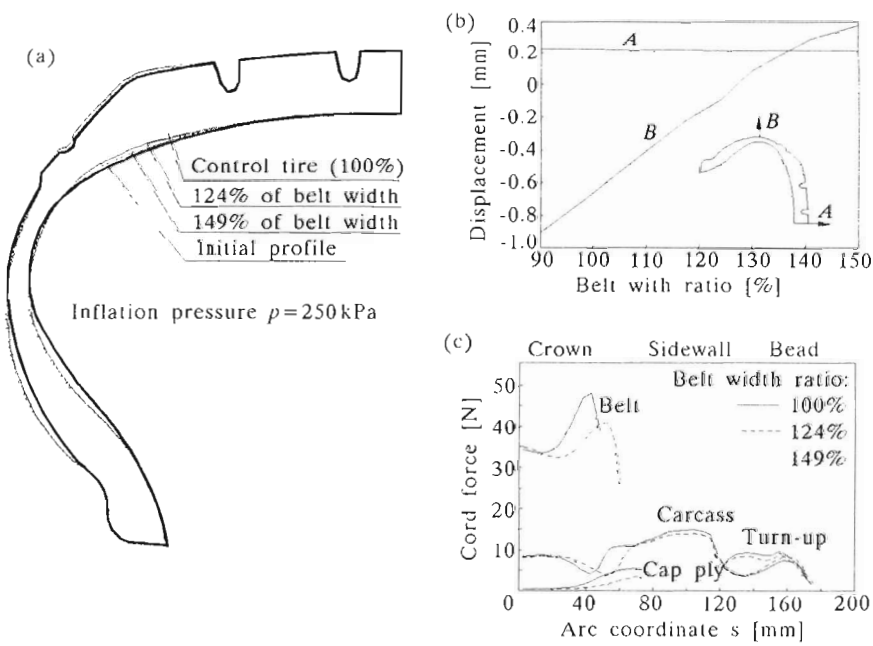

Fig. 7. (a) – Inflated tire profiles, (b) – displacements of the control points, (c) – cord force distribution, for different belt widths, respectively

The belt ply provides a proper tire profile shape and especially a required tread zone curvature in the tire of radial design. A considerable influence of the belt width and cord angle, respectively, on the tire profile after the inflation as well as on the cord force distribution was proved. The initial tire profiles and those after inflation obtained using the FEM approach, for several belt widths are shown in Fig.7a. The belt width variations are expressed in terms of percentage belt width ratios, i.e. the current belt width divided by a control tire belt width. As can be seen from Fig.7b the tire sidewall deformation changes, i.e. decrease in the belt width affects the tire profile

width decrease. Also in the belt edge zone high cord force sensitivity to the belt width variation was found, Fig.7c.

It should be noted that the belt width means in fact an effective belt width. The effective belt width is about 25% smaller than the real one. Fibers in belt plies are not oriented in the circumferential direction, they remain inclined to the equatorial line. Therefore the edge zone of belt has very small stiffness in circumferential direction.

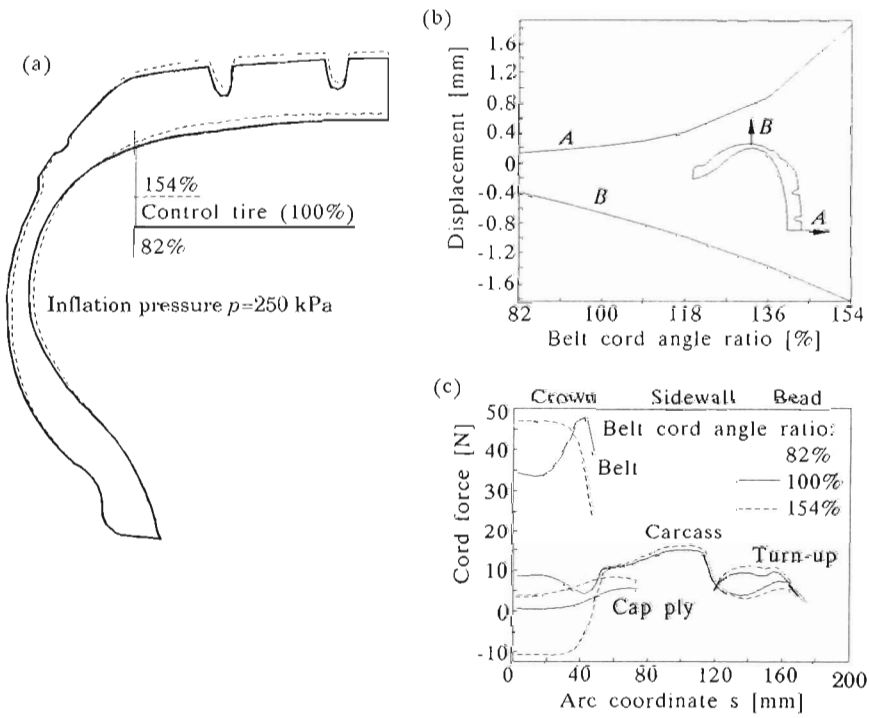

Fig. 8. (a) –Inflated tire profiles, (b) – displacements of the control points, (c) – cord force distribution, for different belt cord angles, respectively

The belt stiffness in circumferential direction is influenced by the cord angle variations. The cord angle is specified by the angle between a fiber direction in a ply and a parallel of the tire building drum. The bigger the angle the larger the radial displacements of tread zone occur after inflation, Fig.8a. Thus, because of considerable meridional stiffness of carcass, the sidewall comes to the inside tire. Displacements of the control points A and B of the tire versus the belt cord angle are plotted in Fig.8b. For an extremely large cord angle the cord forces should take great values to balance the circumferential tension

induced in the tire shell by the inflation pressure, Fig.8c. Since the meridional components of the forces are large, the body ply fibers appear to be even in compression to satisfy the equilibrium. When the angle is small the carcass ply bears a larger part of the meridional tension.

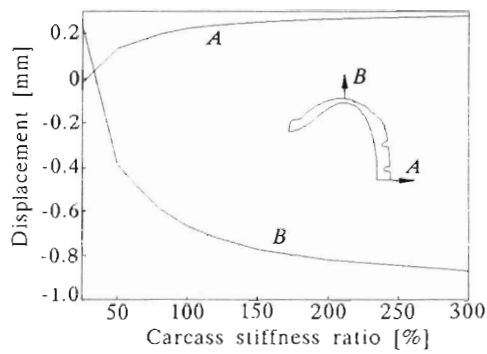

Fig. 9. Displacements of the control points for different carcass fiber stiffnesses

Only a slight influence of the carcass fiber stiffness on the shape of inflated tire profile and the cord force magnitude was detected. Fig.9 shows variations of the control points displacements versus the stiffness ratio of carcass. With the carcass too limp the crown area of the tire may tend to drop inside the tire under inflation pressure. It is undesired phenomenon causing an improper tire contact with pavement what results in non-uniform tread wear.

6. Conclusions

Application of an axisymmetric finite element tire model allows the influence of a lot of pneumatic tire structural parameters on its deformation and stresses upon the inflation pressure to be analysed. A variety of design may be examined with the aid of the model due to its simplicity and thus low cost. Unfortunately, the model can not be applied to the contact problem. This obstacle can be overcome by using a Fourier series expansion for asymmetric contact loading along the circumference.

A sufficient accuracy of the model has been found by comparing the experimental and theoretical results. It is emphasized that adequate belt plies modeling is necessary. Fiber ends of the plies are embedded in flexible rubber and not fixed as in the case of carcass (fibers are anchored around the bead).

As can be seen the presented tire model enable one to evaluate the cord forces distribution among the belt plies and carcass in the crown zone of tire. There was no such a possibility in a net tire model which has been widely used so far.

References

1. BATHE K.J., 1982, *Finite Element Procedures in Engineering Analysis*, Prentice-Hall, Englewood Cliffs, New York
2. CRISFIELD M.A., 1981, A Fast Incremental/Iterative Solution Procedure that Handles "Snapthrough", *Comput. Struct.*, **13**, 55-62
3. DEESKINAZI J., RIDHA R.A., 1982, Finite Element Analysis of Giant eathmover Tires, *Rubb. Chem. Technol.*, **55**, 4, 1044-1054
4. NOOR A.K., TANNER J.A., 1985, Tire Modeling and Contact Problems: Advances and Trends in the Development of Computational Models for Tires, *Comput. Struct.*, **20**, 1-3, 517-533
5. PELC J., 1991, Pneumatic Tire Computational Models – a Survey, (in Polish), *Journal of Theoretical and Applied Mechanics*, **29**, 3-4, 709-725
6. PELC J., 1992, Large Displacements in Tire Inflation Problem, *Enging. Trans.*, **40**, 1, 103-113
7. PELC J., 1994, Stress and Strains in Tractor Radial Tire, (in Polish), *Proc. Conf. on Theory and Technology Development in Technical Modernization of Agriculture*, Olsztyn-Kortowo, 12-15
8. PELC J., 1995, Pre-Processing and Post-Processing in Pneumatic Tire Analysis by the Finite Element Method, *Acta Acad. Agricult. Tech. Olst. Aedificatio et Mechanica*, **26**, 29-37
9. RIDHA R.A., 1980, Computation of Stresses, Strains, and Deformations of Tires, *Rubb. Chem. Technol.*, **53**, 4, 849-902
10. WALTER J.D., PATEL H.P., 1979, Approximate Expressions for the Elastic Constants of Cord-Rubber Laminates, *Rubb. Chem. Technol.*, **52**, 4, 710-724

Analiza parametrów opony pneumatycznej obciążonej ciśnieniem wewnętrznym, za pomocą MES

Streszczenie

Przeanalizowano wpływ niektórych parametrów konstrukcyjnych opony pneumatycznej na jej deformację i naprężenia wywołane działaniem ciśnienia wewnętrznego. Zastosowano metodę elementów skończonych. Założono obrotową symetrię zadania. W rozważaniach uwzględniono duże przemieszczenia. Wzięto także pod uwagę zmienność współczynnika ortotropii w specyficznym kompozycie oponowym złożonym

z kordu i gumy. Zmienne wejściowe stanowiły: szerokość opasania, kąt nachylenia nitki w warstwie opasania i sztywność nitek osnowy. Na podstawie przeprowadzonej weryfikacji modelu obliczeniowego opony można wnioskować, że w zakresie przemieszczeń zadowalająco dokładnie opisuje on obiekt rzeczywisty.

Manuscript received October 8, 1996; accepted for print November 10, 1997